Available online at www.sciencedirect.com
SCIENCE DIRECT®
Journal of Organometallic Chemistry 690 (2005) 3567–3576
Journal of Organometallic Chemistry
www.elsevier.com/locate/jorganchem

Mechanistic studies on the formation of Pt(II) hydroformylation catalysts in imidazolium-based ionic liquids

Peter Illner [a], Achim Zahl [a], Ralph Puchta [a,b], Nico van Eikema Hommes [b], Peter Wasserscheid [c], Rudi van Eldik [a,*]

[a] Institute for Inorganic Chemistry, University of Erlangen-Nürnberg, Egerlandstr. 1, 91058 Erlangen, Germany
[b] Computer Chemistry Center, University of Erlangen-Nürnberg, Nägelsbachstr. 25, 91052 Erlangen, Germany
[c] Department for Chemical Reaction Engineering, University of Erlangen-Nürnberg, Egerlandstr. 3, 91058 Erlangen, Germany

Received 27 January 2005; received in revised from 14 March 2005; accepted 14 March 2005
Available online 5 May 2005

Dedicated to Prof. Rolf W. Saalfrank on the occasion of his 65th birthday

Abstract

The kinetics of the formation of the active species *cis*-$[Pt^{II}(PPh_3)_2Cl(SnCl_3)]$ and *cis*-$[Pt^{II}(PPh_3)_2(SnCl_3)_2]$ from the hydroformylation catalyst precursor *cis*-$[Pt^{II}(PPh_3)_2Cl_2]$ in the presence of $SnCl_2$, was studied in two different imidazolium-based ionic liquids. A large range of different chlorostannate melts consisting of 1-butyl-3-methyl-imidazolium cations and $[Sn_xCl_y]^{(-y+2x)}$ anions with varying molar fraction of $SnCl_2$, were prepared and characterized by ^1H and ^{119}Sn NMR. The observed chemical shifts point to major changes in the composition of the anionic species within the melt. The second ionic liquid employed, viz., 1-butyl-3-methyl-imidazolium-bis(trifluormethylsulfonyl)amide was prepared in a colorless quality that enabled its application in kinetic studies. The concentration and temperature dependence of the substitution of Cl^- by $[SnCl_3]^-$ to yield *cis*-$[Pt^{II}(PPh_3)_2Cl(SnCl_3)]$, could be studied in detail. Theoretical (DFT) calculations were employed to model the reaction progress and to resolve the role of the ionic liquid in the activation of the catalyst. The available results are presented and a plausible mechanism for the formation of the catalytically active species is suggested.

Keywords: Ionic liquids; Kinetic investigations; Platinum(II)-complexes; Hydroformylation; ^{119}Sn NMR

1. Introduction

Ionic liquids are new solvents with outstanding properties that are currently tested and used as reaction media for different kinds of chemical reactions. Many applications have already been developed and new ones are added every day [1–4]. Despite this development, not much research has been performed on the details of the mechanisms of the reactions occurring in these media, and possible changes that are involved in comparison to conventional solvents. Due to the special properties of ionic liquids, changes in reaction mechanisms could occur and may account for some of the observed effects such as the acceleration of reactions or a higher catalyst lifetime [2]. Moreover, some of the ionic liquids can even act as co-catalysts and thus alter the reaction mechanism [2].

In this study we investigated the formation of catalytically active species from *cis*-$[Pt^{II}(PPh_3)_2Cl_2]$, which has already been used in hydroformylation reactions [5,6], in different ionic liquids. In these systems $SnCl_2$ is usually added to the reaction mixture to act as a co-catalyst. On addition of $SnCl_2$ to a solution of *cis*-$[Pt^{II}(PPh_3)_2Cl_2]$, the solution immediately decolors,

* Corresponding author. Tel.: +49 913 185 27350; fax: +49 913 185 27387.
E-mail address: vaneldik@chemie.uni-erlangen.de (R. van Eldik).

0022-328X/$ - see front matter © 2005 Elsevier B.V. All rights reserved.
doi:10.1016/j.jorganchem.2005.03.029

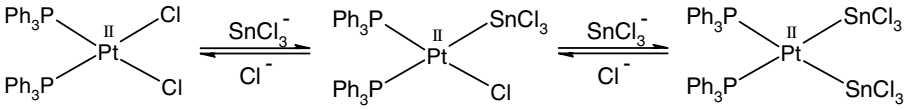

Scheme 1. Formation of the catalytically activate species on addition of $SnCl_2$ to *cis*-$[Pt^{II}(PPh_3)_2Cl_2]$.

indicating the formation of the activated complex which is suggested to be *cis*-$[Pt^{II}(PPh_3)_2Cl(SnCl_3)]$ or *cis*-$[Pt^{II}(PPh_3)_2(SnCl_3)_2]$ depending on the number of $SnCl_2$ molecules inserted into the Pt–Cl bond (see Scheme 1) [7,8]. This aspect was investigated in detail in the present study based on earlier work performed by Wasserscheid and Waffenschmidt [9], in which they studied the performance of the mentioned hydroformylation catalyst in chlorostannate melts. These melts are room temperature ionic liquids consisting of an imidazolium cation and chlorostannate anions (see Scheme 2). The solvent itself can act as a co-catalyst since it consists of chlorostannate anions, which can increase the stability of the catalyst and thereby the resulting overall catalyst activity. We therefore investigated the anion composition of these melts, and possible interactions of these species with the metal complex for the formation of the catalytically active species.

However, insertion of $SnCl_2$ is not the only way in which the activated species can be formed, since substitution of one or both chloride ligands by a $[SnCl_3]^-$ anion is in principle also possible. This was indeed found to be the case for the second ionic liquid studied, viz., 1-butyl-3-methyl-imidazolium-bis(trifluormethylsulfonyl)-amide [bmim][bta] [10,11] (see Scheme 3), a well described ionic liquid with a relatively low viscosity (compared to other ionic liquids) and a melting point below 0 °C. This ionic liquid seemed to be adequate for kinetic investigations once obtained in colorless form after several purification steps (see Section 2). The formation of the catalytically active species was achieved by addition of $[bmim]SnCl_3$ as source of $[SnCl_3]^-$, rather than $SnCl_2$ due to the poor solubility of inorganic salts in this ionic liquid.

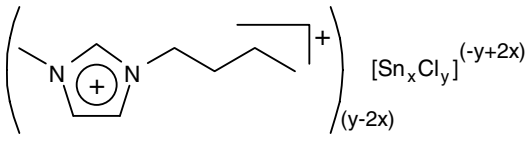

Scheme 2. Structure of the chlorostannate melts.

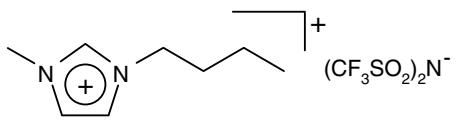

Scheme 3. Structure of [bmim][bta].

2. Experimental

2.1. General remark

In order to prevent hydrolysis of the added Lewis-acid and absorption of air humidity, all reactions and measurements were performed under N_2 atmosphere in well-dried glass apparatus.

2.2. Chlorostannate melts

The used 1-butyl-3-methyl-imidazolium chloride (abbreviated as [bmim]Cl) was purchased from Solvent Innovation and recrystallised from acetone. Water-free $SnCl_2$ was purchased from Acros Organics and used as received. In order to synthesize the melts of different compositions, the necessary amount of $SnCl_2$ was added slowly to [bmim]Cl at 60 °C. On addition the two solids form a pale yellow liquid which is stirred for some hours to ensure complete reaction. Before use, the melts were filtered through a syringe filter (0.2 μm) to obtain optically clean liquids. The melting points of the chlorostannate melts were determined several times by cooling the melts in acetone/dry ice mixtures to about −50 °C and warming them slowly until they reach the melting point.

NMR Spectra were recorded on a Bruker Avance DRX 400WB spectrometer (^1H: 400 MHz; ^{119}Sn: 149 MHz). The chemical shifts are quoted in ppm and refer in case of the proton spectra to TMS as external standard. In case of the ^{119}Sn spectra, pure $SnMe_4$ ($\delta(^{119}Sn) = 0$ ppm) was used as standard. These measurements were recorded using a capillary inside the NMR tube filled with acetone-d_6 to obtain the deuterium field lock. The resulting spectra showed only singlet peaks due to the fast exchange or interconversion of the resulting anions inside the melt, thus not visible on the NMR time scale. UV–Vis spectra were recorded on a Cary 1G spectrophotometer after degassing the solution at 25 °C in silica glass cuvettes.

2.3. 1-Butyl-3-methyl-imidazolium-bis(trifluormethylsulfonyl)amide

1-Butyl-3-methyl-imidazolium-bis(trifluormethylsulfonyl)amide (abbreviated as [bmim][bta]) was synthesized according to a known procedure [10,11] starting from Li(bis(trifluormethylsulfonyl)amide) and [bmim]Cl both purchased from Solvent Innovation and used as received. After drying the resulting pale yellow solvent,

activated charcoal was added and the resulting suspension was stirred for several days. It was filtered using a Millipore filter (pore size 0.2 μm). The almost colorless liquid was washed with double distilled water, dried under vacuum at 60 °C for 2 days and filtered again. ^{1}H NMR (300 MHz; DMSO): $\delta = 9.1$ ppm (s, 1H), $\delta = 7.7$ ppm (d, 2H, $^3J = 9.8$ Hz), $\delta = 4.2$ (t, 2H, $^3J = 7.1$ Hz), $\delta = 3.8$ ppm (s, 3H), $\delta = 1.8$ ppm (m, 2H), $\delta = 1.3$ ppm (m, 2H), $\delta = 0.9$ ppm (t, 3H, $^3J = 7.3$ Hz). UV–Vis spectra were recorded in a tandem cuvette on a Cary 1G spectrophotometer. The water content of this ionic liquid was determined by a Karl-Fischer titration using a Metrohm 756 KF Coulometer and found to be 55 ppm.

3. Results and discussion

3.1. Chlorostannate melts

The synthesis of these ionic liquids was achieved by addition of solid tin(II) chloride to solid 1-butyl-3-methyl-imidazolium chloride at 60 °C, which yielded a melt of yellow color. The two solids are miscible in every molar ratio, giving different liquids of different color, viscosity and melting point. On addition of equimolar amounts of both reactants, $SnCl_2$ that acts as a Lewis acid should react with chloride to give only the $[SnCl_3]^-$ anion. On addition of different ratios of the reactants, different mixtures of anions should be formed. The question to clear is, which of the possible anionic species are formed in which quantities, and how does the composition of the anions in the melt affects the mechanism and the reaction rate of the catalyst activation process.

In order to clarify which anionic species are present in a specific melt, we studied the chemical shift of the ^{119}Sn nuclei and the proton in position 2 (attached to the carbon atom between the two nitrogen atoms) on the imidazolium cation, which is very sensitive to counter ion effects, in chlorostannate melts of varying compositions. With this we extended earlier work done by other groups in chloroaluminate melts [12].

3.1.1. ^{119}Sn NMR Spectra

Following measurements on many melts of different compositions, a correlation between the molar fraction of $SnCl_2$ and the chemical shift was observed (see Fig. 1). Throughout these measurements only a single ^{119}Sn signal was observed. The maximum in the chemical shift of the ^{119}Sn nucleus occurs at an equimolar composition at which $[SnCl_3]^-$ should be the only existing anion. In the concentration range where an excess of $SnCl_2$ is present, viz., $x(SnCl_2) > 0.50$, a linear correlation between the molar ratio of $SnCl_2$ and the decrease in the chemical shift exists, which points to an improved shielding of the Sn nucleus. This suggests the formation of the $[Sn_2Cl_5]^-$ dimer, where electron density can be transferred between the Sn nuclei via the chloride bridge. The linear correlation indicates a complete reaction, which means that for each $SnCl_2$ molecule added the dimer is formed. This gives the opportunity to calculate the amount of the dimer present in a defined melt. On addition of more than a twofold excess of $SnCl_2$, viz., $x(SnCl_2) > 0.66$, the quantity of $SnCl_2$ that exceeds the twofold excess precipitates, which means that no trimer ($[Sn_3Cl_7]^-$) is formed and that the highest molar ratio of $SnCl_2$ achievable is $x(SnCl_2) = 0.66$.

In the concentration range where an excess of imidazolium chloride is present, a sigmoidal curve is observed, which points to an equilibrium between two species that depends on the amount of $SnCl_2$ or Cl^- present in the melt. This could indicate the formation of the $[SnCl_4]^{2-}$ anion [13] in which the Sn nucleus is more shielded due to the higher charge on the anion.

Despite the fact that significantly different $[Sn_xCl_y]^{(-y+2x)}$ species are present in the melts, only a

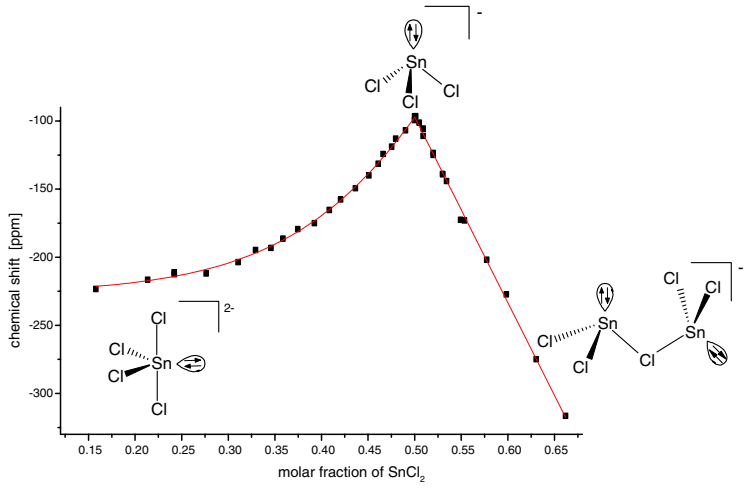

Fig. 1. Chemical shift of the Sn nucleus as a function of the molar fraction of $SnCl_2$ and the proposed anionic species present in the melts.

single ^{119}Sn signal was observed under all conditions, indicating that rapid exchange processes on the NMR time scale must take place in all systems.

3.1.2. ^{1}H NMR Spectra

The correlations observed in the ^{1}H NMR spectra are similar (see Fig. 2). At molar ratios $x(SnCl_2) > 0.5$, an analogous linear dependence of the chemical shift can be observed, but at molar ratios $x(SnCl_2) < 0.5$ the chemical shift decreases to lower fields in contrast to the ^{119}Sn spectra for which the chemical shift increased to higher fields. In order to understand this, one must consider the fact that the proton in position 2 is very counter ion sensitive and undergoes H-bonding with the anions present in the melt. For this reason the proton signal is shifted to higher field when more electron rich dimers ($[Sn_2Cl_5]^-$) are present, since that will lead to shielding of the H nucleus due to the high number of electrons. Naturally, there are not enough dimers present for H-bonding to each imidazolium cation (except in the melt with $x(SnCl_2) = 0.66$), but there is a rapid exchange not visible on the NMR time scale. The low field shift in the concentration range with an excess of [bmim]Cl, where the electron rich $[SnCl_4]^{2-}$ is supposed to be formed, results from the decreasing number of $[SnCl_4]^{2-}$ anions. This anion would surely be a good electron donor, but the concentration of these ions decreases with decreasing molar fraction of $SnCl_2$. At the same time the concentration of Cl^- increases and can compete with the $[SnCl_4]^{2-}$ anion as hydrogen-bonding partner. The maximum of the high field shift was measured in pure [bmim]Cl heated to 70 °C, since its melting point is 65 °C.

3.1.3. Determination of melting points

We determined the melting points of some of the chlorostannate melts and found a significant dependence on the molar ratio of $SnCl_2$. We found an eutectic point for an equimolar composition ($x(SnCl_2) = 0.50$) at −24 to −23 °C (see Fig. 3). The melts with molar fractions of $SnCl_2$ lower and higher than 0.50 all have significantly higher melting points.

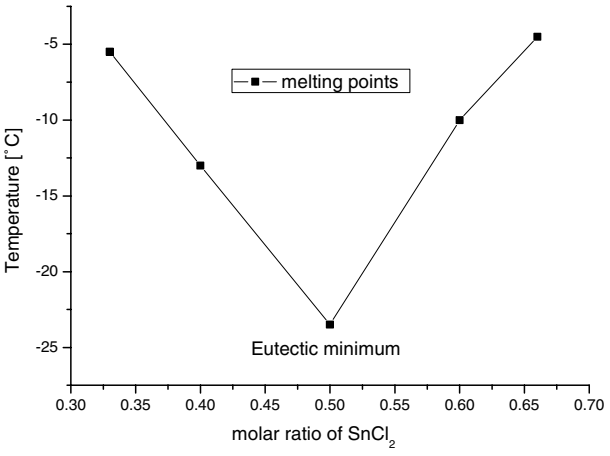

Fig. 3. Melting points of different chlorostannate melts.

3.1.4. Observed UV–Vis spectral changes

On addition of the Pt(II) catalyst to the ionic liquid, the color changes from pale yellow to dark yellow or even red depending on the amount of catalyst added. We performed systematic measurements in chlorostannate melts with the lowest viscosities in the concentration range around $x(SnCl_2) = 0.48$ to 0.55 (typical examples are given in Figs. 4–6).

At a molar ratio of 0.50, a relatively slow reaction can be observed as seen in Fig. 4. If the molar ratio of the melt is higher, a two step reaction results as can be seen in Figs. 5 and 6, respectively. Furthermore, an acceleration of the reaction rate is observed with increasing molar ratio of $SnCl_2$. These effects seem to depend on the

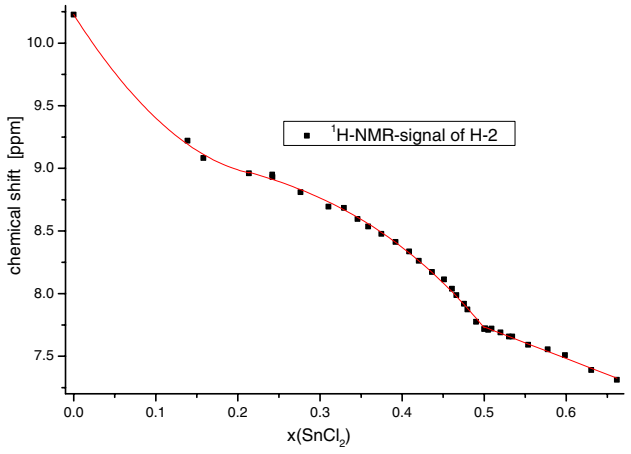

Fig. 2. ^{1}H NMR Shift of H^2 as a function of the molar fraction of $SnCl_2$.

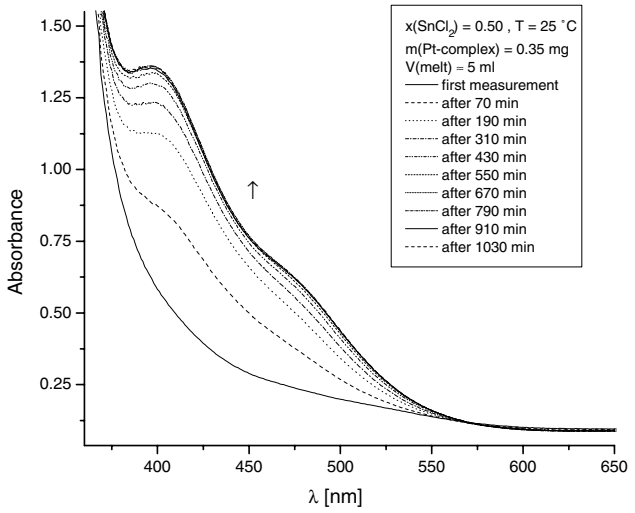

Fig. 4. Observed spectral changes on addition of the Pt(II) complex to a melt of $x(SnCl_2) = 0.50$.

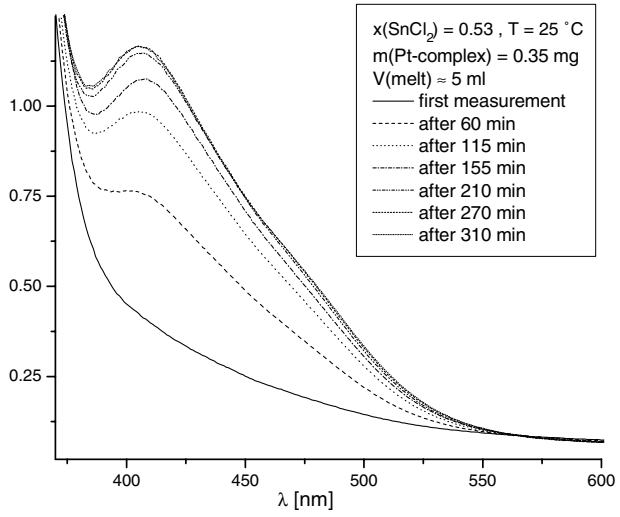

Fig. 5. Observed spectral changes on addition of the Pt(II) complex to a melt of $x(SnCl_2) = 0.53$ (first part).

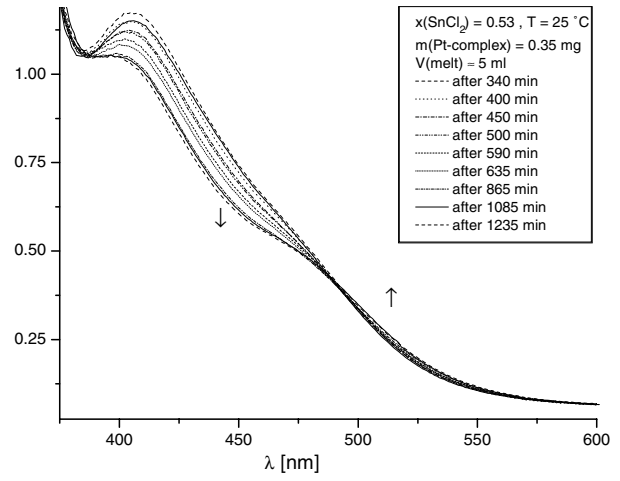

Fig. 6. Observed spectral changes on addition of the Pt(II) complex to a melt of $x(SnCl_2) = 0.53$ (second part).

concentration of the dimer or $SnCl_2$, respectively. Whereas free $SnCl_2$ is not present in the ionic liquid, it should be available in the reaction mixture since our NMR results indicate a rapid exchange of $SnCl_2$ between [bmim]$SnCl_3$ and [bmim]Sn_2Cl_5 [8]. The more $SnCl_2$ present in the ionic liquid, the faster is the insertion into the Pt–Cl bond. Experiments to quantify the concentration dependence of this process have not been performed so far.

Apparently no reaction occurs below a molar ratio of 0.50. The reason could be the absence of free available $SnCl_2$, since below a molar ratio of 0.50 there should only be a rapid exchange of chloride between [bmim]$SnCl_3$ and [bmim]$_2SnCl_4$, such that no insertion reaction can occur.

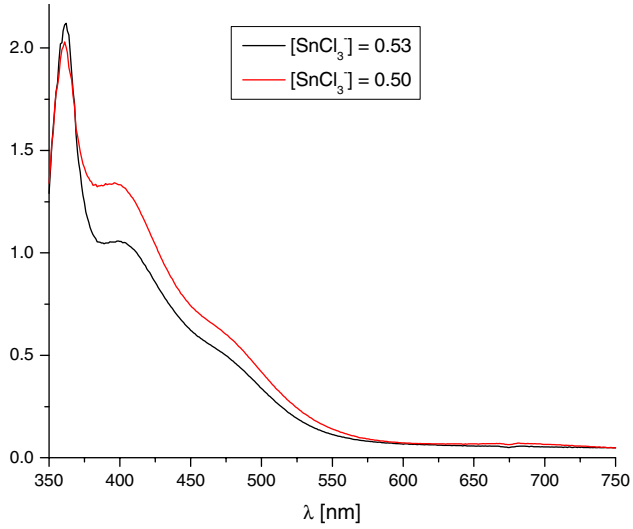

Fig. 7. Observed spectra after 16 h reaction time in melts with $x(SnCl_2) = 0.50$ and $x(SnCl_2) = 0.53$, respectively.

The remaining question is why only a single reaction step is observed at a molar ratio of 0.50 in contrast to the higher molar ratios. The product spectra of the reactions in the melts with compositions of 0.50 and 0.53 are almost exactly the same (see Fig. 7). Thus, the resulting products in both cases should be the same. This indicates that there could be different reaction routes that lead to the same product. Further investigations will be performed to clarify this aspect.

3.2. [bmim][bta]

This ionic liquid [10,11] was purified to a colorless quality such that UV–Vis measurements could be carried out. The absorption above a wavelength of 350 nm was low enough to perform detailed measurements (see Fig. 8). However, one remaining necessity was to

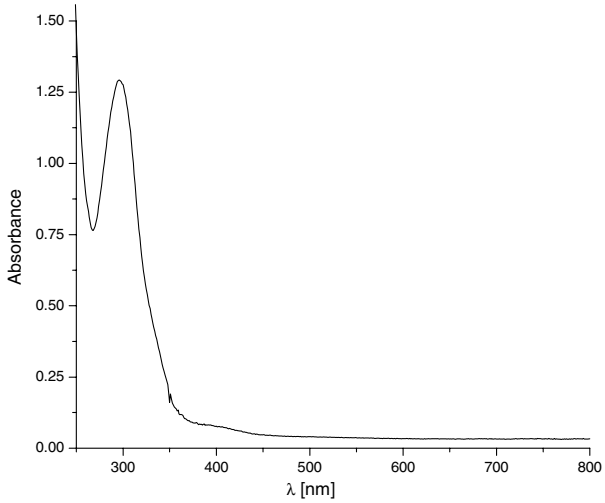

Fig. 8. UV–Vis spectrum of pure [bmim][bta].

reduce the water content of the ionic liquid, which is up to 1.4% (w/w) in water equilibrated [bmim][bta] [11]. The water content can affect the viscosity of the ionic liquid or even act as a potential nucleophile and interfere with the measurements. Furthermore, the solubility of the Pt(II) complex depends on the water content. In addition, $SnCl_2$ can react with water to form insoluble SnCl(OH) which further can disturb the measurements. Therefore, the ionic liquid had to be dried very thoroughly (see Section 2).

A further problem was the poor solubility of polar salts like $SnCl_2$ in this ionic liquid such that another form to create the active species in the melt was needed. Fortunately, the chlorostannate melts described above are soluble in [bmim][bta] and were therefore used to adjust the concentration of $[SnCl_3]^-$, which acts as the attacking nucleophile, in this ionic liquid. The chlorostannate melt used to adjust the $[SnCl_3]^-$ concentration was an equimolar composition of the reactants, $x(SnCl_2) = 0.50$, thus only containing $[SnCl_3]^-$ anions. $[SnCl_3]^-$ was added in at least a tenfold excess as compared to the Pt(II) complex concentration to reach pseudo-first-order conditions. The kinetic measurements were performed at 25 °C at several $[SnCl_3]^-$ concentrations. The observed reaction was found to consist of two steps as shown by the UV–Vis spectra presented in Fig. 9. The first step is relatively fast, shows good first-order behavior (compare Fig. 10), and the observed rate constant depends linearly on the $[SnCl_3]^-$ concentration as shown in Fig. 11 with a second order rate constant calculated to be $k_1 = 0.301 \pm 0.007\ M^{-1}\ s^{-1}$ at 25 °C. The temperature dependence of the reaction was also studied and the results are plotted in Fig. 12 from which it follows that $\Delta H^{\#} = 46.0 \pm 0.8$ kJ mol^{-1} and $\Delta S^{\#} = -100 \pm 3$ J K^{-1} mol^{-1}.

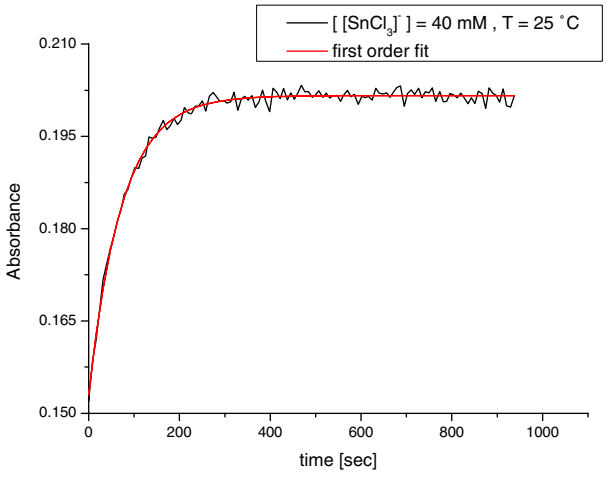

Fig. 10. Typical kinetic trace for the first reaction step in [bmim][bta] at $[[SnCl_3]^-] = 40$ mM.

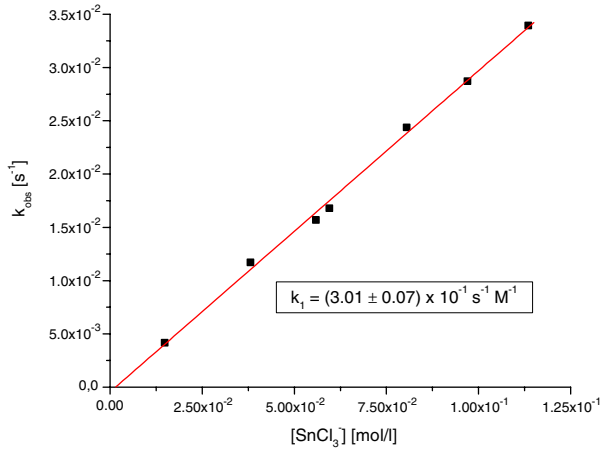

Fig. 11. Observed first order rate constant as a function of the $[SnCl_3]^-$ concentration added to *cis*-$[Pt^{II}(PPh_3)_2Cl_2]$.

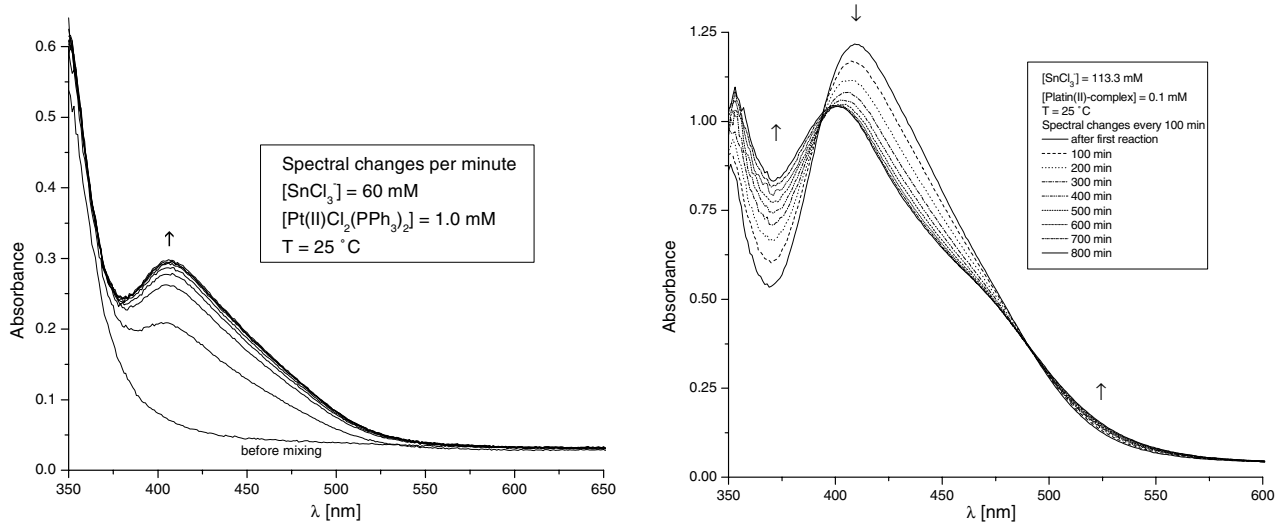

Fig. 9. Spectral changes observed during the first and second reaction steps.

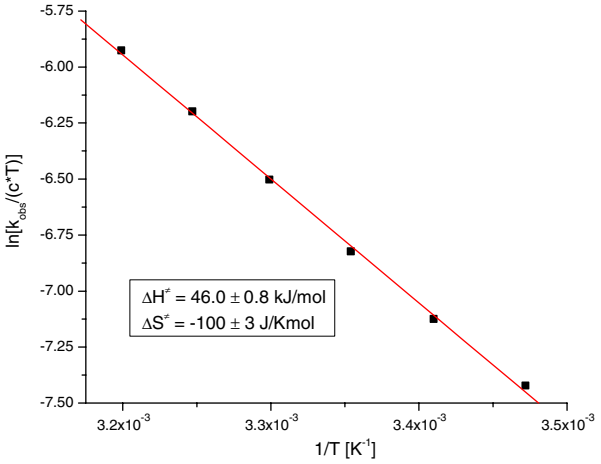

Fig. 12. Temperature dependence of the second order rate constant for the reaction of $[SnCl_3]^-$ with *cis*-$[Pt^{II}(PPh_3)_2Cl_2]$.

The first reaction step is suggested to involve nucleophilic substitution of Cl^- by $[SnCl_3]^-$ as concluded from the linear concentration dependence. It proceeds via an associative mechanism which can be deduced from the very negative activation entropy. So the first reaction step should yield the catalytically active complex *cis*-$[Pt^{II}(PPh_3)_2Cl(SnCl_3)]$.

The second relatively slow reaction was very difficult to study due to the precipitation of side products. Immediately after addition of $[SnCl_3]^-$, the slow formation of a white precipitate (suggested to be Sn(OH)Cl or even $SnCl_2$) was observed, which complicated further monitoring of the slow reaction which has a reaction time of about 24 h. Preliminary results suggest that the second reaction itself consists of two parallel steps, one dependent and one independent of the concentration of $[SnCl_3]^-$. However, a more detailed study is required to resolve the complications referred to above in more detail before any definite mechanistic conclusions can be reached.

In a recent paper, Daguenet and Dyson [14] described the inhibition of the catalytic activity of a Ru(II) complex in ionic liquids in cases where the activating step involved dissociation of a chloride ligand. They found very low solvating interactions between chloride anions and the $[bmim]^+$ cations, thus leading to a higher nucleophilicity of chloride and thus preventing the easy dissociation of chloride from the metal center. If the activation of the metal complex includes such a dissociation step as in the system described above, inhibition of the catalytic activity can occur.

However, in the case of [bmim][bta] the situation is different. The added [bmim]$SnCl_3$ could act as a co-solvent and thus increase the solvation of the chloride to enable dissociation from the metal center. Daguenet and Dyson [14] used water as a co-solvent, but other solvents should work as well. Furthermore, the interaction between the $[bta]^-$ anion, which has a very shielded charge in the center of the anion since the CF_3SO_2 groups provide a "steric block", and the $[bmim]^+$ cation could be even weaker than the interaction between chloride ion and $[bmim]^+$. This favors the solvation and dissociation of chloride in this ionic liquid. If the second possibility is correct, then other catalytic systems that involve chloride dissociation steps could work in this ionic liquid as well, in spite of the presence of $[bmim]^+$(see also theoretical calculations). Daguenet and Dyson [14] checked the inhibition of catalyst activity only in [bmim][CF_3SO_3] and [bmim][BF_4] ionic liquids with anions whose charge is relatively located on the outside of the anion contrary to the $[bta]^-$ anion. It would therefore be interesting to check the activity of their catalyst in [bmim][bta] to see if an inhibition occurs or not.

3.3. Theoretical calculations

Quantum chemical computations nowadays are established as a valuable tool for elucidating reaction mechanisms. We performed hybrid DFT computations at the B3LYP/LANL2DZp level, i.e., with pseudopotentials on the heavy elements and the valence basis set augmented with polarization functions [15] on several species involved in this study [16]. The GAUSSIAN suite of programs was used throughout all the calculations presented here [17]. Corrections for zero point vibrational energy are made. Solvent influences were probed via single point calculations employing the IPCM model [18]. Unfortunately, technical problems prevented these computations for some species, including $SnCl_2$ and $[SnCl_3]^-$. For reasons of computational efficiency, we replaced the PPh_3 ligand on the Pt(II) complex by PH_3 and the butyl side chain on the $[bmim]^+$ moiety by a methyl group (the computed results hence refer to $[mmim]^+$).

Three pathways are conceivable for the formation of *cis*-$[Pt^{II}(PH_3)_2Cl(SnCl_3)]$:

(i) substitution of Cl^- by $[SnCl_3]^-$,
(ii) substitution of Cl^- by $[Sn_2Cl_5]^-$, followed by further reaction,
(iii) insertion of $SnCl_2$ in a Pt–Cl bond.

Reaction (i) was computed to proceed as shown in Fig. 13. First, a precursor complex between *cis*-$[Pt^{II}(PH_3)_2Cl_2]$ and $[SnCl_3]^-$ is formed. The computed gas phase interaction energy of 25 kcal/mol is exaggerated; IPCM calculations were not possible. The Pt–Sn distance is almost 6 Å, i.e., no bonds are present between *cis*-$[Pt^{II}(PH_3)_2Cl_2]$ and $[SnCl_3]^-$. In the transition state structure for the substitution process, the Pt–Sn bond is already well established (2.74 Å) whereas the Pt–Cl bond (2.57 Å) is not yet significantly disrupted. This indicates a high degree of associative character. An activation barrier of 20 kcal/mol was

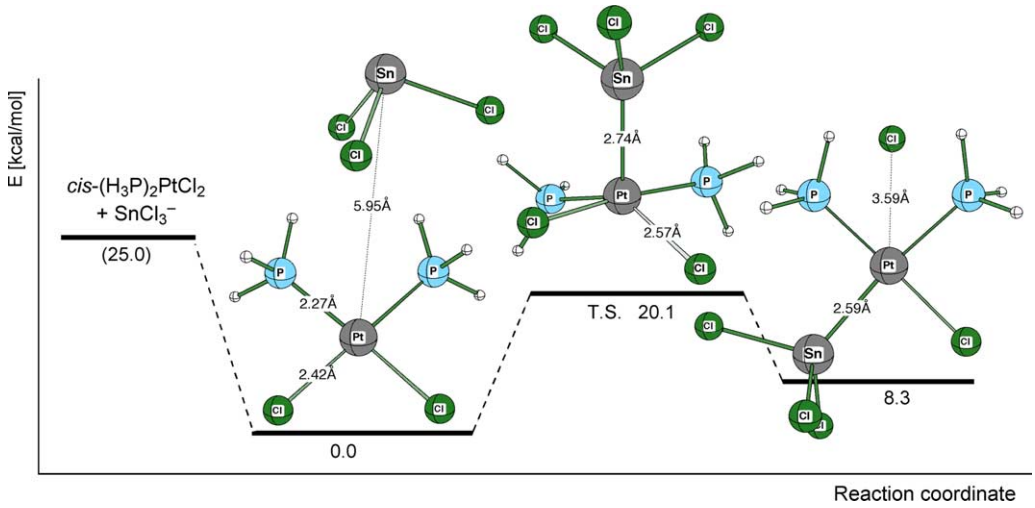

Fig. 13. Calculated reaction pathway for the reaction of *cis*-$[Pt^{II}(PH_3)_2Cl_2]$ with $[SnCl_3]^-$.

calculated. In the product complex, the chloride anion is bound electrostatically at a distance of 3.6 Å. To separate *cis*-$[Pt^{II}(PH_3)_2Cl(SnCl_3)]$ and Cl^- in the gas phase requires almost 50 kcal/mol. Correction for solvent influences lowers this value to 16.7 kcal/mol.

In order to evaluate the overall energetics of the reaction, we avoided the technical difficulties (vide supra) as well as the problems associated with huge electrostatic interaction energies by considering the reaction

$$[\text{mmim}]SnCl_3 + [Pt^{II}(PH_3)_2Cl_2] \rightarrow [\text{mmim}]Cl + [Pt^{II}(PPh_3)_2Cl(SnCl_3)]$$

Interestingly, we computed this reaction to be endothermic. The gas phase reaction energy is +12.6 kcal/mol. However, inclusion of solvent effects reduces this to +5.1 kcal/mol. We expect this value still to be too high; the computations were done using gas phase optimized structures and employing the rather simplified IPCM model that does not include specific solvent–solute interactions. For comparison, the energy difference between precursor and product complex is computed to be +8.3 kcal/mol.

Preliminary results for reaction (ii) showed very similar behavior as for reaction (i). Therefore, this pathway was not pursued any further at present.

A significantly different picture emerges for reaction (iii) as shown in Fig. 14. *cis*-$[Pt^{II}(PH_3)_2Cl_2]$ and $SnCl_2$ form a strongly bound precursor complex which is 18.7 kcal/mol more stable than the separated reactants. The interaction energy stems from the newly formed Sn–Cl bond, which is computed to be 2.73 Å, only slightly longer than the bridging Sn–Cl bond in $[Sn_2Cl_5]^-$ (2.67 Å). The reaction proceeds through a

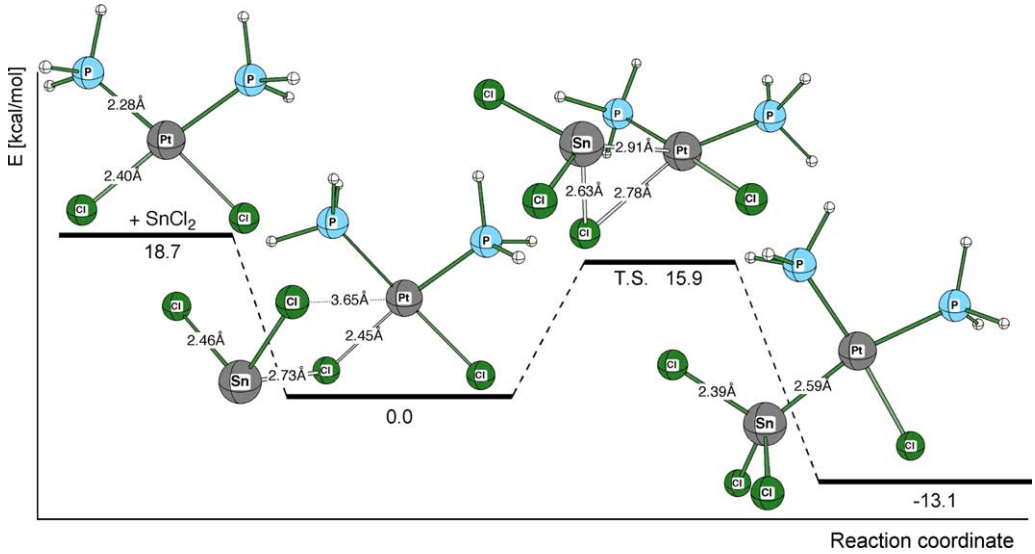

Fig. 14. Calculated reaction pathway for the reaction of *cis*-$[Pt^{II}(PH_3)_2Cl_2]$ with $SnCl_2$.

tightly bound three-center transition structure. The gas phase activation barrier of 16 kcal/mol is lower than the value computed for reaction (i); inclusion of solvent effects via the IPCM model lowers the barrier to 9.0 kcal/mol. The overall reaction is exothermic: the product, $[Pt^{II}(PH_3)_2Cl(SnCl_3)]$, is 13 kcal/mol (IPCM: 10.3 kcal/mol) more stable than the precursor complex and 32 kcal/mol more stable than the separated reactants.

Based on the above, we conclude that formation of $[Pt^{II}(PPh_3)_2Cl(SnCl_3)]$ in chlorostannate melts with $x(SnCl_2) > 0.50$ most probably proceeds via insertion of $SnCl_2$ in a Pt–Cl bond. As mentioned above, free $SnCl_2$ is not present in the ionic liquid, but it should be available in the reaction mixture since our NMR results indicate a rapid exchange of $SnCl_2$ between [bmim]$SnCl_3$ and [bmim]Sn_2Cl_5 [8]. This can clearly be seen from the fact that only a single ^{119}Sn signal is observed in the employed melts.

On the other hand, the formation of $[Pt^{II}(PPh_3)_2Cl(SnCl_3)]$ via the reaction of *cis*-$[Pt^{II}(PPh_3)_2Cl_2]$ with [bmim]$SnCl_3$ in [bmim][bta] must proceed via substitution of Cl^- by $[SnCl3]^-$, since no $SnCl_2$ is available under those conditions. In contrast with the observations made by Daguenet and Dyson [14], we find that this reaction proceeds very well, although it involves, in the final reaction step, abstraction of chloride. However, in our case, Cl^- is abstracted from a negatively charged species and $[mmim]^+$ is present as counter ion. Furthermore, model computations on [mmim][bta], [mmim]$SnCl_3$, and [mmim]Cl indicate the latter to be the most stable species. Exchange of the anion by chloride is exothermic in both reactions:

$$[mmim][bta] + Cl^- \rightarrow [mmim]Cl + [bta]^- \quad -27.4\ \text{kcal/mol}$$

$$[mmim]SnCl_3 + Cl^- \rightarrow [mmim]Cl + [SnCl_3]^- \quad -21.2\ \text{kcal/mol}$$

Bonding between the $[bmim]^+$ and $[bta]^-$ moieties is not strong, such that [bmim][bta] is likely to be present as separated ion pairs. This should further favor the abstraction of Cl^- in this solvent.

4. Conclusions

The possibility to perform systematic kinetic studies in the room temperature ionic liquids studied could be demonstrated. We were able to observe the addition of $SnCl_2$ or $[SnCl_3]^-$ to the Pt(II) catalyst according to a two step mechanism in both ionic liquids. The formation of $[Pt^{II}(PPh_3)_2Cl(SnCl_3)]$ is suggested to occur in the first reaction step and was studied in terms of its concentration and temperature dependence in [bmim][bta]. In the chlorostannate melts, an increase in reaction rate of this first step was observed that correlated with the molar fraction of $SnCl_2$ in the melt. The second reaction step is suggested to involve the formation of $[Pt^{II}(PPh_3)_2(SnCl_3)_2]$ and is considerably slower than the first step. Theoretical calculations underline the validity of the mechanistic conclusions. The $[bmim]^+$ cations show a strong tendency to bind Cl^-; this can assist the activation of the catalyst.

Acknowledgments

The authors gratefully acknowledge financial support from the Deutsche Forschungsgemeinschaft, Fonds der Chemischen Industrie, Max-Buchner Forschungsstiftung and the European Commission within the framework of the RTN Contract No. MRTN-CT-2003-503864. Prof. Tim Clark, Computer Chemistry Center, is kindly acknowledged for his support of this work. We thank the Regionales Rechenzentrum Erlangen (RRZE) for a generous allotment of computer time.

References

[1] T. Welton, Coord. Chem. Rev. 248 (2004) 21–2459.
[2] J. Dupont, R.F. deSouza, P.A.Z. Suarez, Chem. Rev. 102 (2002) 3667.
[3] M. Maase, Chem. Unserer Zeit 38 (2004) 434.
[4] M. Volland, V. Seitz, M. Maase, M. Flores, R. Papp, K. Massonne, V. Stegmann, K. Halbritter, R. Noe, M. Bartsch, W. Siegel, M. Becker, O. Huttenloch, (BASF AG), WO 2003/062251,200.
[5] R.L. Pruett, Adv. Organomet. Chem. 17 (1979) 1.
[6] P.H. Meessen, Dissertation RWTH Aachen, 1997.
[7] A. Scrivanti, A. Berton, L. Toniolo, C. Botteghi, J. Organomet. Chem. 314 (1986) 369.
[8] M. Gomez, G. Muller, D. Sainz, J. Sales, Organometallics 10 (1991) 4036.
[9] P. Wasserscheid, H. Waffenschmidt, J. Mol. Catal. A: Chem. 164 (2000) 61–67.
[10] J.G. Huddleston, A.E. Visser, W.M. Reichert, H.D. Willauer, G.A. Broker, R.D. Rogers, Green Chem. 3 (2001) 156–164.
[11] P. Bonhôte, A. Dias, N. Papageorgiou, K. Kalyanasundaram, M. Grätzel, Inorg. Chem. 35 (1996) 1168–1178.
[12] J.S. Wilkes, J.A. Levisky, J.L. Pflug, C.L. Hussey, T.B. Scheffler, Anal. Chem. 54 (1982) 2378–2379.
[13] B. Müller, T.M. Seward, Geochim. Acta 65 (2001) 4187–4199.
[14] C. Daguenet, P.J. Dyson, Organometallics 23 (2004) 6080–6083.
[15] (a) A.D. Becke, J. Phys. Chem. 97 (1993) 5648–5652;
(b) C. Lee, W. Yang, R.G. Parr, Phys. Rev. B 37 (1988) 785–789;
(c) P.J. Stephens, F.J. Devlin, C.F. Chabalowski, M.J. Frisch, J. Phys. Chem. 98 (1994) 11623–11627;
(d) T.H. Dunning Jr., P.J. Hay, Mod. Theor. Chem. 3 (1976) 1–28;
(e) P.J. Hay, W.R. Wadt, J. Chem. Phys. 82 (1985) 270–283;
(f) P.J. Hay, W.R. Wadt, J. Chem. Phys. 82 (1985) 284–298;
(g) P.J. Hay, W.R. Wadt, J. Chem. Phys. 82 (1985) 299–310;
(h) S. Huzinaga (Ed.), Gaussian Basis Sets for Molecular Calculations, Elsevier, Amsterdam, 1984.
[16] The performance of the computational level employed in this study is well documented, see for example: S. Klaus, H. Neumann, H. Jiao, A. Jacobi von Wangelin, D. Gördes, D. Strübing, S.

Hübner, M. Hately, C. Weckbecker, K. Huthmacher, T. Riermeier, M. Beller, J. Organomet. Chem. 689 (2004) 3685–3700;
R.W. Saalfrank, C.h. Deutscher, H. Maid, A.M. Ako, S. Sperner, T. Nakajima, W. Bauer, F. Hampel, B.A. Heß, N.J.R. van Eikema Hommes, R. Puchta, F.W. Heinemann, Chem. Eur. J. 10 (2004) 1899–1905.

[17] M.J. Frisch, G.W. Trucks, H.B. Schlegel, G.E. Scuseria, M.A. Robb, J.R. Cheeseman, J.A. Montgomery Jr., T. Vreven, K.N. Kudin, J.C. Burant, J.M. Millam, S.S. Iyengar, J. Tomasi, V. Barone, B. Mennucci, M. Cossi, G. Scalmani, N. Rega, G.A. Petersson, H. Nakatsuji, M. Hada, M. Ehara, K. Toyota, R. Fukuda, J. Hasegawa, M. Ishida, T. Nakajima, Y. Honda, O. Kitao, H. Nakai, M. Klene, X. Li, J.E. Knox, H.P. Hratchian, J.B. Cross, V. Bakken, C. Adamo, J. Jaramillo, R. Gomperts, R.E. Stratmann, O. Yazyev, A.J. Austin, R. Cammi, C. Pomelli, J.W. Ochterski, P.Y. Ayala, K. Morokuma, G.A. Voth, P. Salvador, J.J. Dannenberg, V.G. Zakrzewski, S. Dapprich, A.D. Daniels, M.C. Strain, O. Farkas, D.K. Malick, A.D. Rabuck, K. Raghavachari, J.B. Foresman, J.V. Ortiz, Q. Cui, A.G. Baboul, S. Clifford, J. Cioslowski, B.B. Stefanov, G. Liu, A. Liashenko, P. Piskorz, I. Komaromi, R.L. Martin, D.J. Fox, T. Keith, M.A. Al-Laham, C.Y. Peng, A. Nanayakkara, M. Challacombe, P.M.W. Gill, B. Johnson, W. Chen, M.W. Wong, C. Gonzalez, J.A. Pople, GAUSSIAN 03, Revision B.03, Gaussian Inc., Wallingford, CT, 2004.

[18] J.B. Foresman, T.A. Keith, K.B. Wiberg, J. Snoonian, M.J. Frisch, J. Phys. Chem. 100 (1996) 16098–16104 (The default $\varepsilon = 78.39$ was used throughout).